Imbalance Difference Model for Common-Mode Radiation From Printed Circuit Boards

Changyi Su, *Student Member, IEEE*, and Todd H. Hubing, *Fellow, IEEE*

***Abstract*—The differential-mode signals in printed circuit board (PCB) traces are unlikely to produce significant amounts of radiated emissions directly; however these signals may induce common-mode currents on attached cables, enclosures, or heat sinks that result in radiated electromagnetic (EM) interference. Full-wave EM modeling can be performed in order to determine the level of radiated emissions produced by a PCB, but this modeling is computationally demanding and does not provide the physical insight necessary to explain how differential signals induce common-mode currents on distant objects. This paper describes a model for determining the common-mode currents on cables attached to a PCB that is based on the concept of *imbalance difference*. The imbalance difference model is derived from research that shows that changes in geometrical imbalance cause differential-to common-mode conversion. This paper applies an imbalance difference model to PCB structures and compares the resulting equivalent source configurations to those obtained with traditional voltage- and current-driven models, as well as full-structure simulations.**

***Index Terms*—Common-mode radiation, electromagnetic (EM) coupling, imbalance difference model, printed circuit board (PCB).**

I. Introduction

COMMON-MODE currents are much more likely to generate significant levels of unintentional radiated emissions than differential-mode currents [1]. Signal traces on printed circuit boards (PCBs) carry differential currents by design, but the signals on these traces can couple to larger nearby objects, such as heat sinks, enclosures, and attached cables. The common-mode currents induced on these larger objects can be significant source of radiated emissions.

For simple PCB structures, the radiated emissions can be calculated using full-wave numerical modeling codes. However, this approach is limited by the complexity of the models and the extensive computational resources required to analyze the details of each trace structure. In addition, brute-force modeling of the entire board provides relatively little physical insight into the electromagnetic interference (EMI) source mechanisms. Alternatively, an effective equivalent model can be obtained by eliminating sources and differential signal structures that do not contribute significantly to the radiated emissions and focusing on the features that could possibly be significant sources of EMI. Equivalent models are generally much simpler than model-everything full-wave models and provide physical insight into the board features that have the greatest impact on radiated emissions.

Two equivalent models analyzing the differential-mode to common-mode conversion in PCBs were introduced in a 1994 paper [2]. These models are commonly referred to as *current-driven* and *voltage-driven* sources, referring to the prominent differential signal parameter affecting the common-mode currents induced on the external structures. The current-driven mechanism refers to common-mode currents induced by the signal currents returning in the "ground" structure causing voltage differences between objects referenced to different parts of the structure [2]–[4]. The voltage-driven mechanism refers to electric field coupling from traces or heat sinks that are at one potential to cables or other external objects that are at a different potential [5]–[7]. An equivalent wire antenna model for estimating voltage-driven common-mode currents was developed in [5]. In this model, the common-mode voltage source is placed at the junction between the ground plane and the attached cable. The magnitude of the equivalent voltage source is expressed in terms of the ratio of the self-capacitances of the board and the trace or heat sink.

These equivalent models are typically applied in situations, where it is assumed that one coupling mechanism is dominant. However, for trace-and-board geometries, common-mode currents due to the electric and the magnetic field coupling coexist and can be comparable in strength. Therefore, it is desirable to model the coupling between the differential signals on the board and the common-mode currents on attached cables without specifying a particular field coupling mechanism. In this paper, an equivalent model based on the concept of imbalance difference [8], [9] is described. The imbalance difference model is another way of describing how differential-mode signals are converted to common-mode voltages and currents, based on changes in the degree of imbalance in PCB transmission systems. Using a parameter called the *current-division factor* or *imbalance parameter*, the magnitude and location of equivalent common-mode sources can be derived quantitatively. These common-mode sources then replace all of the differential signal structures on the PCB. This paper demonstrates the application of the imbalance difference model to PCB circuit structures and compares the models obtained to current- and voltage-driven models and to full-wave simulations of the entire board structure.

II. Description of the Imbalance Difference Model

In 2000, a paper by Watanabe *et al.* [8] demonstrated that geometrical imbalance in a circuit does not necessarily result in

Manuscript received January 3, 2010; revised March 27, 2010; accepted April 24, 2010. Date of current version February 16, 2011.

The authors are with the Clemson University, Clemson, SC 29635 USA (e-mail: csu@clemson.edu; t.hubing@ieee.org).

Color versions of one or more of the figures in this paper are available online at http://ieeexplore.ieee.org.

Digital Object Identifier 10.1109/TEMC.2010.2049853

0018-9375/$26.00 © 2010 IEEE

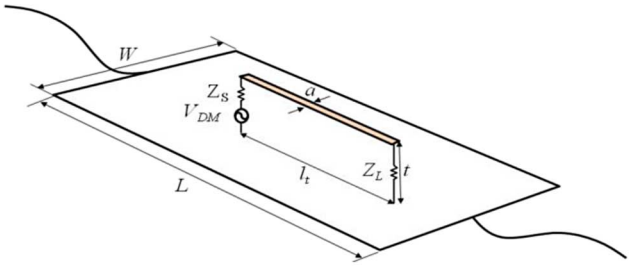

Fig. 1. Trace-board structure with cables attached to the ground plane.

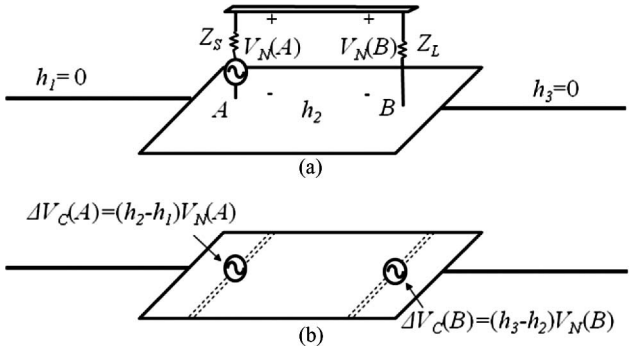

Fig. 2. Imbalance difference model. (a) Trace-and-board configuration. (b) Equivalent model.

differential-mode to common-mode conversion. Instead, it was proposed that *changes* in the imbalance are responsible. Watanabe *et al.* introduced a method for quantifying the imbalance in a given transmission-line structure and showed that it was possible to characterize the differential- to common-mode conversion by introducing equivalent common-mode voltage sources at points where there was a change in the imbalance. This idea was subsequently developed in a number of other publications [9]–[15] and has proven to be a powerful tool for the design and modeling of PCB structures.

In order to illustrate how this concept can be applied to PCBs with attached cables, consider the structure shown in Fig. 1. Fig. 1 schematically shows a simple circuit board structure with a signal trace routed over a solid ground plane. The board has cables attached to both ends that are referenced to the ground plane. The microstrip trace is driven at one end and terminated at the other end. The trace-board geometry is electrically small at low frequencies, where common-mode currents induced on the cables are likely to be the dominant source of radiated emissions. The space between the trace and the ground plane is filled with a dielectric material with a dielectric constant ε_r and a thickness *t*. In Fig. 1, the thickness *t* is exaggerated for clarity. In most practical structures, *t* is several orders of magnitude smaller than *L* and *W*.

An imbalance parameter can be defined for any transmission-line geometry. The imbalance parameter is a number between 0 and 0.5, where a perfectly balanced structure (e.g., two symmetric conductors with identical cross sections) has an imbalance parameter of 0.5. Perfectly unbalanced structures (e.g., a coaxial cable or a trace over an infinite ground plane) have imbalance parameters equal to 0. The imbalance parameter, denoted as "*h*" in this paper, is dependent on the cross-sectional structure of the transmission line, and therefore, changes when two transmission lines with different cross sections are connected.

The change in the imbalance at the interconnection can be used to define an equivalent common-mode voltage source for the purpose of modeling the common-mode currents induced on the structure. Using Fig. 2 as an example, there is a change in the imbalance parameter *h* at both ends of the microstrip. At each end, the width of the trace varies from a finite value *a* to zero. At the discontinuity points *A* and *B*, as shown in Fig. 2(a), common-mode voltages are generated in the ground plane and their magnitudes are computed as the product of the differential-mode voltage and the change in the imbalance parameter [9]

$$\Delta V_C(x) = \Delta h\, V_N(x) \tag{1}$$

where V_N is the differential-mode voltage between the signal trace and the return plane, and x denotes the location of the common-mode excitation. According to (1), the common-mode excitation at location *A* is computed as follows:

$$\Delta V_C(A) = (h_2 - h_1)\, V_N(A) \tag{2}$$

and the common-mode excitation at *B* is as follows:

$$\Delta V_C(B) = (h_3 - h_2)\, V_N(B). \tag{3}$$

The common-mode equivalent geometry is excited by $\Delta V_c(A)$ and $\Delta V_c(B)$, which are placed on the board at points *A* and *B*, as shown in Fig. 2(b), respectively.

As indicated in (2) and (3), the relationship between the differential-mode and common-mode source amplitudes is completely determined by the change in the imbalance parameter. The imbalance parameter *h* is defined as follows:

$$h = \frac{I_{\text{CM-signal}}}{I_{\text{CM}}} \tag{4}$$

where I_{CM} and $I_{\text{CM-signal}}$ are the total common-mode current and the common-mode current flowing on the signal trace, respectively. For microstrip trace structures, this parameter is given by [12]

$$h = \frac{C_{\text{trace}}}{C_{\text{trace}} + C_{\text{board}}} \tag{5}$$

where C_{trace} and C_{board} are the stray capacitances per unit length of the signal trace and the ground plane, respectively. Stray capacitance does not include the mutual capacitance between the trace and ground plane and is represented by the lines of electric flux that originate on the trace or the board and terminate at infinity. Equation (5) was derived from the telegrapher's equations with the assumption that only the TEM mode propagates on each transmission line. The line capacitance per unit length can be extracted numerically using a 2-D electrostatic or quasi-static code. In this paper, QuickField Students' version [16], a free 2-D finite-element code, was used to compute the capacitances in all simulations presented in Section IV.

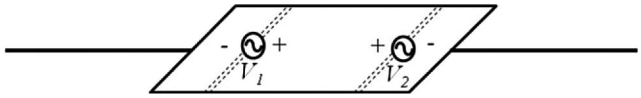

Fig. 3. Imbalance difference model for the trace-board configuration in Fig. 1.

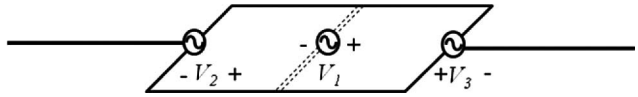

Fig. 4. Equivalent model based on the current- and voltage-driven models.

The imbalance parameter for the portions of the structure extending beyond the trace is zero. The imbalance parameter for the trace-board portion h_2 must always be between 0 and 0.5. Since h_1 and h_3 are zero, the common-mode voltages in (2) and (3) can be rewritten as follows:

$$V_{\mathrm{CM}}(A) = h_2 V_N(A) \tag{6}$$

and

$$V_{\mathrm{CM}}(B) = -h_2 V_N(B). \tag{7}$$

An important restriction on the use of this modeling approach is that the cross section of the board-trace configuration must be small relative to a wavelength; otherwise the imbalance factor is not well defined. This restriction also applies to traditional voltage- and current-driven models.

III. Imbalance Difference Compared to Voltage- and Current-Driven Models

A. Imbalance Difference Model for the Trace-Board Configuration

Fig. 3 illustrates the imbalance difference model for the trace-board configuration of Fig. 1 after the trace and differential-mode source have been replaced by the equivalent common-mode sources. Expressed as a function of the trace current, the magnitude of the differential-mode voltage between the trace and the ground plane at point *A* in Fig. 1 is as follows:

$$V_N(A) = \left| j2\pi f L_{\mathrm{trace}} I_{\mathrm{DM}} + Z_L I_{\mathrm{DM}} \right|. \tag{8}$$

Combining (5), (6), and (8), the equivalent common-mode voltage at point *A* is as follows:

$$V_1 = \left| jh2\pi f L_{\mathrm{trace}} I_{\mathrm{DM}} + hZ_L I_{\mathrm{DM}} \right| \tag{9}$$

where I_{DM} is the differential-mode current. Taking the differential-mode current as a reference, the phasor expression for the common-mode voltage is as follows:

$$\begin{aligned} V_1 &= h2\pi f L_{\mathrm{trace}} I_{\mathrm{DM}} \angle 90^\circ + hZ_L I_{\mathrm{DM}} \angle 0^\circ \\ &\approx h2\pi f L_{\mathrm{trace}} I_{\mathrm{DM}} \angle 90^\circ + h\frac{Z_L}{Z_S + Z_L} V_{\mathrm{DM}} \angle 0^\circ. \end{aligned} \tag{10}$$

Similarly, the equivalent common-mode voltage at point B is given by

$$V_2 = h\frac{Z_L}{Z_S + Z_L} V_{\mathrm{DM}}. \tag{11}$$

From (10) and (11), the equivalent model consists of two parts. One part is the first term in (10), which is proportional to the differential-mode current. The other part is the second term in (10) and (11), which is proportional to the differential-mode voltage.

B. Voltage- and Current-Driven Models for the Trace-Board Configuration

It is interesting to compare the imbalance difference model to a combination of the current-driven model [3] and the voltage-driven model [5], as shown in Fig. 4. In the current-driven model, one equivalent voltage source is placed at the midpoint of the current return path on the board. The magnitude of the source is proportional to the differential-mode current flowing through the trace

$$V_1 = 2\pi f L_{\mathrm{return}} I_{\mathrm{DM}} \tag{12}$$

where L_{return} is the partial inductance of the return plane [4]

$$L_{\mathrm{return}} = \frac{\mu_0}{\pi}\frac{tl_t}{W}\frac{1}{\sqrt{1 - 4\left(1 - 2t/W\right)\left(s/W\right)^2}}, \tag{13}$$

s is the offset of the trace from the center of the board, and *t*, l_t, *W* are the trace height, the trace length, and the board width, as shown in Fig. 1, respectively.

In the voltage-driven model, equivalent voltage sources are placed at the junctions between the cables and the plane. The magnitudes of the voltage sources are expressed in terms of the ratio of the self-capacitances of the board and the trace

$$V_2 = V_3 = \frac{C_{\mathrm{trace}}}{C_{\mathrm{board}}}\frac{Z_L}{Z_S + Z_L} V_{\mathrm{DM}}. \tag{14}$$

Although the two equivalent models (see Figs. 3 and 4) differ in the number, the locations, and the magnitudes of the equivalent sources, they are both approximately equivalent to the original trace-board configuration. It is demonstrated in the next section that the predicted radiated emissions using the two models produce similar results at frequencies up to 500 MHz.

C. Equivalent Models for Shorted- and Open-Trace Configurations

A shorted-trace configuration, as illustrated in Fig. 5, is a special case of Fig. 2(a) that enhances the current-driven coupling and suppresses the voltage-driven coupling to the cables. At point *A*, the equivalent common-mode voltage is given by (2)

$$\begin{aligned} V_{\mathrm{CM}} &= h_2 V_N(A) \\ &= \frac{C_{\mathrm{trace}}}{C_{\mathrm{trace}} + C_{\mathrm{board}}} 2\pi f L_{\mathrm{trace}} I_{\mathrm{DM}}. \end{aligned} \tag{15}$$

The loop inductance causes the differential current I_{DM} to lag the differential-mode voltage V_{DM}. Assuming the phasor of

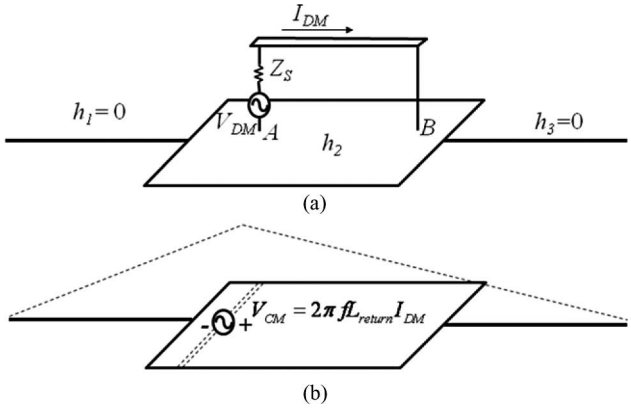

Fig. 5. Imbalance difference model for the shorted-trace structure.

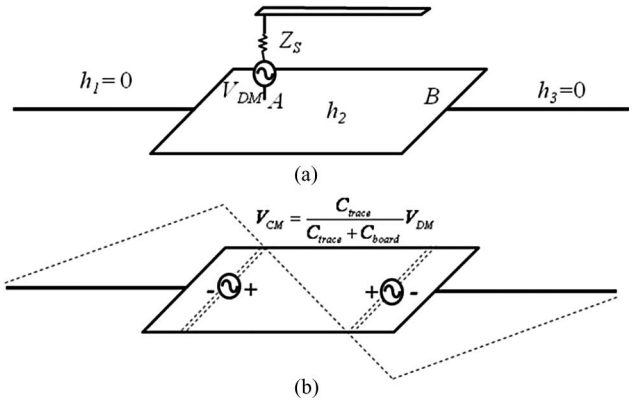

Fig. 6. Imbalance difference model for the open-circuit structure.

the differential current is $I_{\rm DM}\angle 0^\circ$, the common-mode voltage in (15) can be expressed using phasor notation as follows:

$$V_{\rm CM} = 2\pi f L_{\rm trace} \frac{C_{\rm trace}}{C_{\rm trace} + C_{\rm board}} I_{\rm DM}\angle 90^\circ. \qquad (16)$$

The trace is shorted to the ground plane at the load side; so according to (3), the magnitude of the equivalent common-mode excitation at point *B* is zero

$$\Delta V_C\,(B) = -h_2 V_N(B) = 0. \qquad (17)$$

To enhance the voltage-driven coupling and suppress the current-driven coupling to the cables, the load end of the trace is open-circuited, as shown in Fig. 6(a). Since the imbalance parameter is independent of the loading condition, (5) is still valid for the open-circuit case. Therefore, the magnitude of the equivalent common-mode voltage is as follows:

$$V_{\rm CM} = \frac{C_{\rm trace}}{C_{\rm trace} + C_{\rm board}} V_{\rm DM}. \qquad (18)$$

Two common-mode voltage sources are placed on the return plane. These sources have the same magnitude, but opposite phase.

The equivalent antenna model for the open-circuit geometry is shown in Fig. 6(b). In the imbalance difference model of the open-circuit geometry, two common-mode voltage sources are placed at points *A* and *B*, respectively. They have the same magnitude, but opposite phases. Hence, the common-mode current distribution is mirrored across the center of the board.

It is noted that the current-driven mechanism induces common-mode currents that flow in the same direction on the two cables, while the voltage-driven mechanism induces common-mode currents that flow in opposite directions on the two cables. Therefore, when both mechanisms are significant, the total common-mode current will not be the same on both wires.

IV. Modeling Examples

A. Trace Terminated With 50 Ω

To evaluate the imbalance difference models described in the previous section, numerical simulations of the trace-board configuration in Fig. 1 were performed. The maximum radiated electric fields at a distance of 3 m were calculated for both the original configuration (modeling the entire trace-board structure) and the equivalent common-mode models (i.e., the imbalance difference model, current-driven model, and voltage-driven model). The simulations were performed using a full-wave EM modeling code based on the method of moments [17].

The board dimensions were 10 cm × *W* cm, where *W* was the width of the board. A 5-cm-long, 1-mm-wide trace was placed 3 mm above the plane, and two 50-cm cables were attached to the board and oriented horizontally. A 2-V source with a 50-Ω series impedance was connected between one end of the trace and the ground plane. The other end of the trace was terminated by a 50-Ω resistor. The board was located in free space.

Fig. 7 shows the maximum radiated electric fields obtained from 4-cm and 10-cm-wide boards. The solid curves include the maximum radiation obtained from a full-wave model of the entire configuration. As indicated by (5), the imbalance parameter can be reduced by widening the ground plane. Hence, the common-mode radiated emissions from the 10-cm-wide board are about 8 dB lower than the emissions from the 4-cm-wide board. This observation is consistent with the experimental results in [3].

In Fig. 7, the dashed lines and dashed–dotted lines represent the results obtained from the imbalance difference model in Fig. 3 and the voltage/current-driven model in Fig. 4, respectively. Both equivalent models yield results that are in reasonable agreement with the original configuration, particularly near the resonant peaks.

B. Trace Terminated With 0 Ω

The imbalance difference model eliminates the need to make assumptions about which source model is dominant in a given situation. To illustrate the value of this, the geometry in the previous section was modeled with the trace shorted to the ground plane at the load. The source amplitude was 2 V and the source impedance was 100 Ω. This is a configuration where the current-driven mechanism might be expected to dominate. The current is

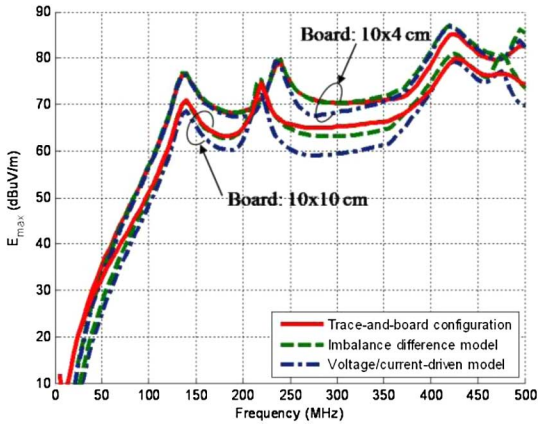

Fig. 7. Comparison of the radiated emissions from the full trace-board configuration and the two equivalent models.

approximately the same as it was in the 50-Ω load configuration, but the voltage is significantly reduced.

The maximum 3-m radiation from 4-cm and 10-cm-wide boards was calculated using the imbalance difference model and compared to results obtained by analyzing the original trace-board configuration. The emissions from the shorted-trace configuration are shown in Fig. 8(a). The solid line is the result obtained from analysis of the complete trace-board structure. The dashed line represents the simulation result for the imbalance difference model. The magnitude of the equivalent common-mode voltage was computed using (15). Fig. 8(b) compares the maximum electric field radiated from the open-circuited board using both the original model and the imbalance difference model. In this case, the magnitudes of the equivalent common-mode excitations were computed using (18).

The simulation results in Fig. 9 show that both the imbalance model and the current-driven model calculate the maximum radiation from the shorted-trace configurations with reasonable accuracy. However, the current-driven model fails to predict the small peaks at 235 and 495 MHz for the 10 cm × 4 cm boards, and at 215 and 475 MHz for the 10 cm × 10 cm boards. Further analysis shows that these peaks are caused by the voltage difference between the trace and the ground plane, which is zero at the load, but nonzero away from the load due to the inductance of the trace. Although the current-driven peaks are dominant, the voltage-driven mechanism cannot be neglected, even when the signal trace is shorted to the ground plane.

C. Trace Located Near the Board Edge

It has been demonstrated experimentally and through numerical modeling that the radiated fields are higher when signal traces are located near the board edge. Berg *et al.* [18] explained that the increment in the radiated emissions is the result of increased magnetic flux beneath the board. Explained in terms of the imbalance difference model described in Section III, the imbalance parameter of the trace-board pair increases as the trace is moved toward the board edge.

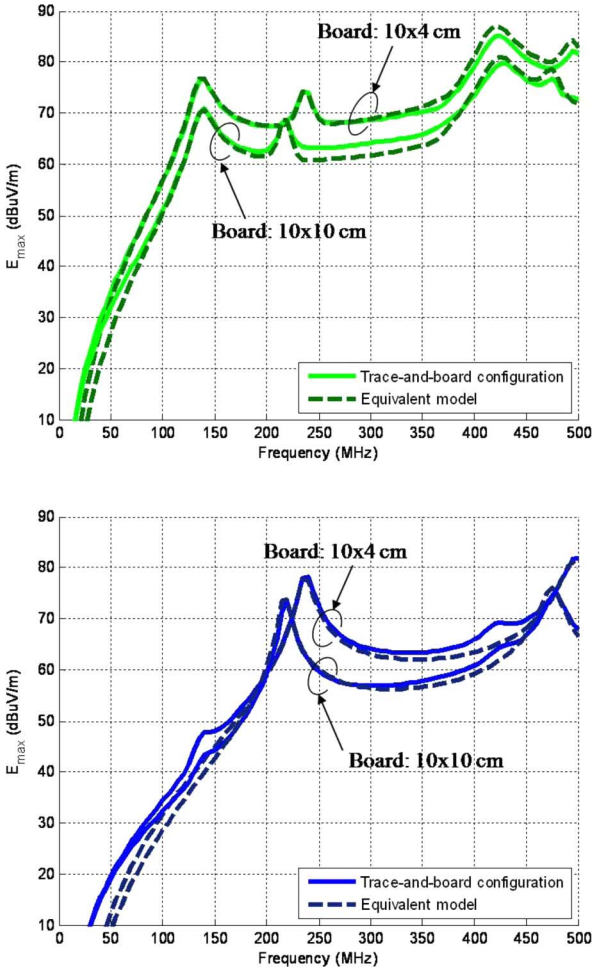

Fig. 8. Comparison of the radiated emissions calculated using the trace-board configuration and the imbalance difference model from shorted trace (upper plot) and open trace (lower plot).

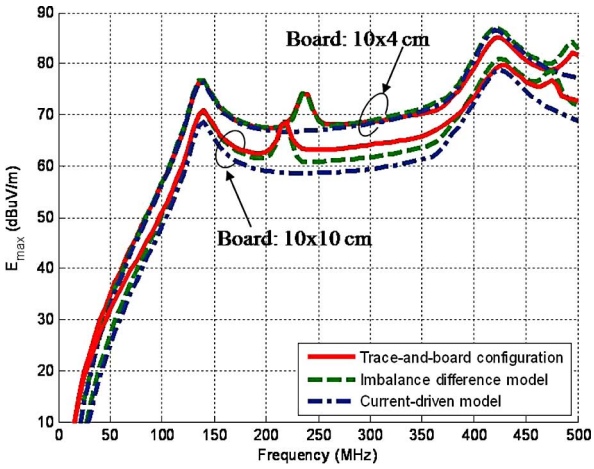

Fig. 9. Comparison of the radiated emissions from the shorted-trace configuration calculated using the imbalance difference model and current-driven model.

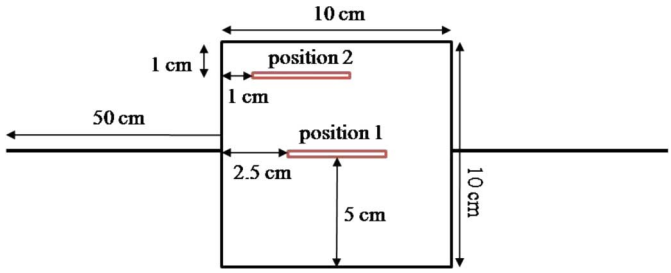

Fig. 10. Test-board configuration with different trace positions.

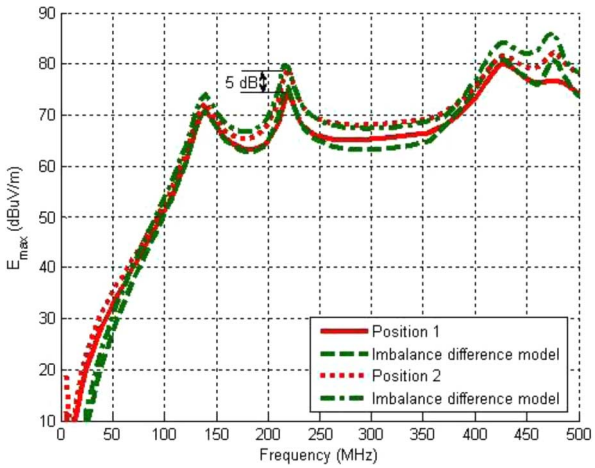

Fig. 11. Comparison of radiated fields from the full trace-board configuration and the imbalance difference model for two trace positions.

To illustrate this, boards were evaluated with different trace positions. Fig. 10 shows a 10 cm $\times$ 10 cm board with a cable attached to each side. A 1-mm-wide, 5-cm-long trace is located 3 mm above the ground plane. Two different trace positions were evaluated. The maximum radiated fields from the board are shown in Fig. 11. The simulation results show that the radiated field is stronger when the trace is near the board edge. The imbalance parameter is 0.0236 for the trace at position 1 and 0.0341 for the trace at position 2, resulting in a 5 dB difference at 220 MHz. The imbalance difference model results are similar to the full trace-and-board configuration results over the entire frequency range evaluated.

V. Conclusion

The imbalance difference model can be used to estimate the radiated emissions from trace-board structures due to common-mode currents induced on attached cables. The results obtained are similar to results obtained using voltage- and current-driven models. Both models produce accurate results even though they employ equivalent sources that have different amplitudes and locations. The voltage- and current-driven models have the advantage that they are more intuitively linked to the field coupling responsible for the induced currents. However, by observing the amplitudes of the terms in (10) and (11), the imbalance difference model also provides useful information about the relative importance of the electric and magnetic field coupling. Furthermore, the imbalance difference model has the advantage that it is simpler to implement and models both electric and magnetic field coupling simultaneously.

References

[1] C. R. Paul, *Introduction to Electromagnetic Compatibility*. New York: Wiley, 1992.

[2] J. L. Drewniak, T. H. Hubing, and T. P. Van Doren, "Investigation of fundamental mechanisms of common-mode radiation from printed circuit boards with attached cables," in *Proc. IEEE Int. Symp. Electromagn. Compat.*, Chicago, IL, Aug. 1994, pp. 110–115.

[3] D. M. Hockanson, J. L. Drewniak, T. H. Hubing, T. P. Van Doren, F. Sha, and M. Wilhelm, "Investigation of fundamental EMI source mechanisms driving common-mode radiation from printed circuit boards with attached cables," *IEEE Trans. Electromagn. Compat.*, vol. 38, no. 4, pp. 557–566, Nov. 1996.

[4] M. Leone, "Design expressions for trace-to-edge common-mode inductance of a printed circuit board," *IEEE Trans. Electromagn. Compat.*, vol. 43, no. 4, pp. 667–671, Nov. 2001.

[5] H. Shim and T. Hubing, "Model for estimating radiated emissions from a printed circuit board with attached cables driven by voltage-driven sources," *IEEE Trans. Electromagn. Compat.*, vol. 47, no. 4, pp. 899–907, Nov. 2005.

[6] H. Shim and T. Hubing, "Derivation of a closed-form expression for the self-capacitance of a printed circuit board trace," *IEEE Trans. Electromagn. Compat.*, vol. 47, no. 4, pp. 1004–1008, Nov. 2005.

[7] S. Deng, T. Hubing, and D. Beetner, "Estimating maximum radiated emissions from printed circuit boards with an attached cable," *IEEE Trans. Electromagn. Compat.*, vol. 50, no. 1, pp. 215–218, Feb. 2008.

[8] T. Watanabe, O. Wada, T. Miyashita, and R. Koga, "Common-mode-current generation caused by difference of unbalance of transmission lines on a printed circuit board with narrow ground pattern," *IEICE Trans. Commun.*, vol. E83-B, no. 3, pp. 593–599, Mar. 2000.

[9] T. Watanabe, O. Wada, Y. Toyota, and R. Koga, "Estimation of common-mode EMI caused by a signal line in the vicinity of ground edge on a PCB," in *Proc. IEEE Int. Symp. Electromagn. Compat.*, Minneapolis, MN, Aug. 2002, pp. 113–118.

[10] T. Watanabe, S. Matsunaga, O. Wada, M. Kishimoto, T. Tanimoto, A. Namba, and R. Koga, "Equivalence of two calculation methods for common-mode excitation on a printed circuit board with narrow ground plane," in *Proc. IEEE Int. Symp. Electromagn. Compat.*, Boston, MA, Aug. 2003, pp. 22–27.

[11] O. Wada, "Modeling and simulation of unintended electromagnetic emission from digital circuits," *IEICE Trans. Commun.* (Japanese Edition), vol. 87, no. 8, pp. 1062–1069, Jul. 2003.

[12] T. Watanabe, H. Fujihara, O. Wada, Y. Toyota, R. Koga, and Y. Kami, "A prediction method of common-mode excitation on a printed circuit board having a signal trace near the ground edge," *IEICE Trans. Commun.*, vol. E87-B, no. 8, pp. 2327–2334, Aug. 2004.

[13] Y. Toyota, A. Sadatoshi, T. Watanabe, K. Iokibe, R. Koga, and O. Wada, "Prediction of electromagnetic emissions from PCBs with interconnections through common-mode antenna model," in *Proc. IEEE Int. Symp. Electromagn. Compat.*, Zurich, Switzerland, Sep. 2007, pp. 107–110.

[14] Y. Toyota, T. Matsushima, K. Iokibe, R. Koga, and T. Watanabe, "Experimental validation of imbalance difference model to estimate common-mode excitation in PCBs," in *Proc. IEEE Int. Symp. Electromagn. Compat.*, Detroit, MI, Aug. 2008, pp. 1–6.

[15] T. Matsushima, T. Watanabe, Y. Toyota, R. Koga, and O. Wada, "Evaluation of EMI reduction effect of guard traces based on imbalance difference model," *IEICE Trans. Commun.*, vol. E92-B, no. 6, pp. 2193–2200, Jun. 2009.

[16] QuickField Students' version 5.6. (2008, Oct.). [Online]. Available: http://www.quickfield.com/free_soft.htm.

[17] *FEKO User's Manual,* Suite 5.5, Electromagnetic Software and Systems, Stellenbosch, South Africa, Jul. 2009.

[18] D. Berg, M. Tanaka, Y. Ji, X. Ye, J. Drewniak, T. Hubing, R. DuBroff, and T. Van Doren, "FDTD and FEM/MOM modeling of EMI resulting from a trace near a PCB edge," in *Proc. IEEE Int. Symp. Electromagn. Compat.*, Washington, DC, Aug. 2000, pp. 135–140.

Changyi Su (S'08) received the B.Eng. degree from Xian University of Technology, Xian, China, and the M.Eng. degree from Nanyang Technological University, Singapore, in 1993 and 2001, respectively. She is currently working toward the Ph.D. degree from Clemson University, Clemson, SC.

Her current research interests include electromagnetic modeling and computational electromagnetics.

Todd H. Hubing (S'82–M'82–SM'93–F'06) received the B.S.E.E. degree from Massachusetts Institute of Technology, Cambridge, CA, in 1980, the M.S.E.E. degree from Purdue University, West Lafayette, IN, in 1982, and the Ph.D. degree in electrical engineering from the North Carolina State University, Raleigh, NC, in 1988.

From 1982 to 1989, he was in the Electromagnetic Compatibility (EMC) Laboratory, IBM Communications Products Division, Research Triangle Park, NC. In 1989, he was a Faculty Member at the University of Missouri-Rolla, Rolla, MO, where he was engaged in analyzing and developing solutions for a wide range of EMC problems affecting the electronics industry. In 2006, he joined as the Michelin Professor at Clemson University, Clemson, SC for vehicular electronics, where he is involved in EMC and computational electromagnetic modeling, particularly as it is applied to automotive and aerospace electronics.

Prof. Hubing is a Past President of the IEEE Electromagnetic Compatibility Society. He has been involved as the Vice President with the Communication Services Society. He is a Fellow of the Applied Computational Electromagnetic Society.